JEE Journal of Ecological Engineering

Journal of Ecological Engineering, 2027, 28(1), 455–469
https://doi.org/10.12911/22998993/242700
ISSN 2299–8993, License CC-BY 4.0

Received: 2026.10.27
Accepted: 2026.11.16
Published: 2026.12.01

Environmentally friendly synthesis of mesostructured cellular foam silica from palm oil boiler ash for enzyme immobilization

Lilis Hermida[1], Joni Agustian[1*], Darmansyah[1], Aisya Destania Putri[1], Pranesti Dara Dinanti[1], Diah Agita Putri[1], Muhammad Febrian Putra Adha Bren[1]

[1] Department of Chemical Engineering, Universitas Lampung, Jl. Prof S. Brodjonegoro No. 1, Gedong Meneng, Rajabasa, Bandar-Lampung, 35145, Indonesia
* Corresponding author's e-mail: joni.agustian@eng.unila.ac.id

ABSTRACT

Mesostructured cellular foam (MCF) silica is commonly prepared from tetraethyl orthosilicate, which is an imported chemical in Indonesia. To substitute this chemical, palm oil boiler ash (POBA), a locally sourced and environmentally friendly material, was used as replacement. Based-on this alternative, acetic acid and potassium chloride were utilized rather than hydrochloric acid solution and mesitylene, so that a green synthetic process could be developed. The experiments involved conversion of POBA to MCF silica through an extraction process with dilute sulfuric acid solution, formation of sodium silicate using sodium hydroxide, and synthesis of MCF silica from sodium silicate, where the process factors were varied during the experiments. The SiO_2 content in POBA was low, but it increased to 52.838% (w/w) after the extraction. The content of more than 75% (w/w) was obtained after treatment with NaOH. The optimum MCF silica had specific surface area of 738.976 m^2/g, specific pore volume of 2.046 cm^3/g, pore cell diameter of 167.114 Å, and pore window diameter of 97.757 Å. The product was developed by 40 mL of 3M sodium hydroxide, 5 grams of Pluronic® P123, 4.4 mL of acetic acid, and 5 grams of potassium chloride. Effects of the operational factors were observed during synthesis. Immobilization efficiency of glucoamylase enzyme was found as high as 73.33% resulted at temperature of 35 °C, Sorensen phosphate buffer pH of 6.0, initial free enzyme concentration of 8% (w/v), and stirring speed of 120 rpm. Hydrolytic capability of immobilized glucoamylase was observed at different temperature to give the maximum dextrose equivalent (DE) value of 56.61% (w/w) (tapioca substrate) and 15.37% (w/w) (sorghum substrate), at the optimum temperature of 70 °C. These results were lower compared to free glucoamylase DE value, which produced DE value of > 80% (w/w).

Keywords: palm oil boiler ash, MCF silica, factors of synthesis, glucoamylase immobilization, starch hydrolysis

INTRODUCTION

Production of steam in a palm oil mill boiler using palm fibers and shells as fuels produces abundant and renewable combustion ash known as palm oil boiler ash (POBA). POBA is usually disposed of in areas surrounding the mill. If POBA is not treated properly, it can cause environmental and health problem (Asyri et al., 2015; Bagus, 2023). The fine and light ash makes it easily carried away by wind, thus impairing vision and health (Yoescha, 2007). Analysis of POBA indicates that it contains a significant level of silica (SiO_2) compound (Putri et al., 2025; Bukit et al., 2022). Hence, POBA can be used as an alternative source of mesoporous silica to drive the circular economy of palm oil industry.

One such mesoporous silica is mesostructured cellular foam (MCF) silica. This silica is an excellent material for incorporation of catalysts or immobilization of enzymes due to its large pore size and surface area, which enhance diffusion of reactants and products (Piumetti et al., 2012; Chunguang et al., 2010). Previously, it had been applied as supports for urea (Ginting, et al., 2018; Rugayah, et al., 2019; Sriagung, et al., 2021), nickel catalyst (Hermida et al., 2013a,b; Hermida et al., 2016), α-amylase (Agustian and

Hermida, 2024, 2019), and glucoamylase (Agustian and Hermida, 2019b,c, 2018). Until nowadays, this matrix is commonly developed from tetraethyl orthosilicate (TEOS) (Hermida et al., 2013a,b; Hermida et al., 2019; Agudelo et al., 2020; Agudelo et al., 2022; Agustian and Hermida, 2024; Kummamuru et al., 2024).

In Indonesia, TEOS is an imported chemical, similar to other compounds used to prepare the TEOS-derived MCF silica like mesitylene (1,3,5-trimethylbenzene (TMB)) and Pluronic® P123. Hence, they are not easily available. Moreover, the process to produce the TEOS-derived MCF silica involves the use of hydrochloric acid (HCl) solution, which is a corrosive substance, though it is used at a low molarity value (i.e. 1.6 M) (Agustian and Hermida, 2018; Agustian and Hermida, 2019a,b,c). Therefore, substituting TEOS, hydrochloric acid, and mesitylene with locally easily available materials and environmentally friendly chemicals is a significant, challenging, and innovative attempt.

Recently, the MCF silica has been synthesized from bagasse bottom ash (BBA) by modifying the TEOS-derived MCF silica route. The route employed potassium chloride (KCl) salt to replace the TMB as the expansion agent (Agustian and Hermida, 2025). Though the pore diameter size of the BBA-derived MCF silica was smaller than the TEOS-derived MCF silica, the salt-based route was considered as a prospective process as it still developed a type IV mesoporous silica material, but required further efforts to optimize the process.

Conversion of POBA into the MCF silica is an urgent innovation and a new alternative process due to a large number and continuous production of the ash, hence the raw material to prepare the silica is continuously available, and the absence of method(s) for preparing the MCF silica from POBA. This novel route would function the low-value materials. For example, potassium chloride salt is a cheap product that could be used as the expansion agent instead of TMB in order to lower the costs associated with the MCF silica synthesis. Moreover, to create an acidic condition during this synthesis, acetic acid was used to replace HCl solution as explained previously (Choi et al., 2015). Therefore, the research was conducted to develop the POBA-derived MCF silica by substituting the employed materials from the POBA extraction step to the templating agent. As the MCF silica can be used to form immobilized amylases (Agustian and Hermida, 2019a,b,c, 2024), experiments were made on immobilisation of glucoamylase on this matrix to observe its capability as an enzyme matrix.

MATERIALS AND METHODS

Materials

POBA was donated by a local palm oil factory. Pluronic® P-123 (96%) was supplied by Sigma-Aldrich, while potassium chloride (KCl, >99%), potassium dihydrogen phosphate (KH_2PO_4, 100%), and acetic acid (98%) were Merck products. Sodium hydroxide (NaOH, 96%), disodium hydrogen phosphate dodecahydrate ($Na_2HPO_4.12H_2O$, 98%) were bought from Pudak. All chemicals were obtained from domestic suppliers. Sulfuric acid (H_2SO_4, 98%) was acquired from a local company. Reverse osmosis (RO) water was used to dissolved solid chemicals. Glucoamylase was a product from China, theoretically contains 100,000 U/g. Pierce™ bicinchoninic acid (BCA) protein assay kit, used to observe the immobilization process, was a Thermo Scientific product. Tapioca and sorghum starch was bought from a local supermarket. These materials were used directly without any pretreatment.

Synthesis of MCF silica

Initially, POBA was crushed using mortar and then sieved to obtain 200 mesh size solids (Figure 1). Then, 50 grams of the 200-mesh sieved POBA was placed into a glass beaker containing a diluted sulfuric acid solution (500 mL of RO water and 5 mL of H_2SO_4). The mixture was stirred at speed of 100 rpm for 30 minutes, then it was filtered to obtain a solid residue that was subsequently washed with RO water until pH of filtrate reached 7.0 (Figure 1). The washed residue was dried at temperature of 105°C for 4 hours, followed by its calcination at 550°C for 6 hours.

Subsequently, the sodium silicate solution (Na_2SiO_3) was prepared as follows: 9 grams of the calcined POBA and 3 M NaOH (its volume was shown in Table 1) were mixed in a glass beaker. The mixture was stirred at speed of 100 rpm for 30 minutes and then heated in an 80°C water bath for 4 hours. Afterward, the mixture was filtered to isolate the solids required for production of the MCF silica. Finally, the MCF silica was synthesized following methodologies outlined by

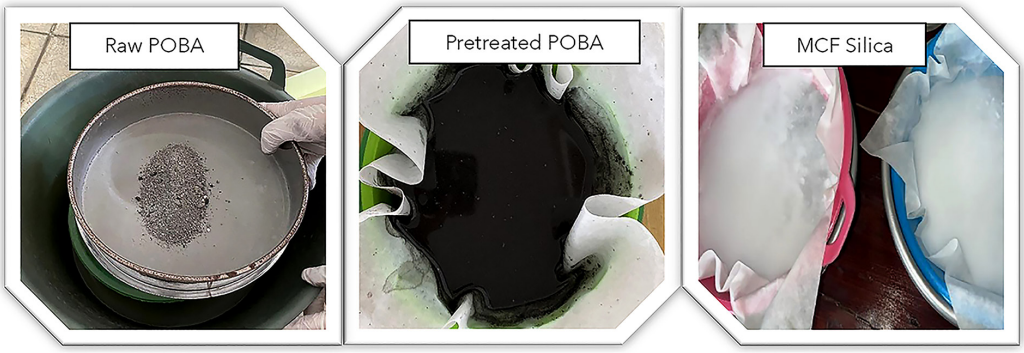

Figure 1. Raw POBA, pretreated POBA, and MCF silica

Table 1. Design of experiment

Process	Variable	Value	Unit
Synthesis of MCF silica	NaOH	40; 50; 60	mL
	Pluronic P123	4; 5; 6	g
	KCl	5; 7.5; 10; 15	g
	Ch_3COOH	2.2; 3.3; 4.4	mL
Immobilization of enzyme	Temperature	25; 30; 40	°C
	pH	4.5; 5; 5.5	---
	Enzyme concentration	8; 9; 10	mg/mL
	Agitation speed	100; 120; 140	rpm

Hermida et al. (2013a,b), Choi et al. (2015), and Agustian and Hermida (2025), by replacing tetraethyl orthosilicate with Na_2SiO_3. The process commenced with dissolution of Pluronic P123 (refer to Table 1) in 100 mL of RO water, which contained 2.2-4.4 mL of 98% acetic acid, at room temperature. KCl was put into the mixture with its quantity as indicated in Table 1. The resulting mixture was subjected to heating at 60°C while being stirred at 750 rpm for one hour. 8 mL of sodium silicate was introduced into the mixture under high-speed stirring (1000 rpm) for duration of five minutes. The mixture was heated in a water bath at 60°C for 20 hours. After this, the aging process was conducted in the water bath at 80°C for 72 hours. The mixture was filtered and rinsed with RO water until the filtrate reached a pH of 7.0. The white solids were dried at 100°C for 12 hours, followed by their calcination at 550°C for six hours to yield the MCF silica.

Enzyme immobilization and starch hydrolysis

Enzyme immobilization: An amount of free glucoamylase as given in Table 2 was dissolved in 30 mL of 100 mM Sorensen phosphate buffer solution. Then, 0.5 grams of MCF silica was put into the enzyme solution. The mixture was shaken in a water-bath shaker for 5 hours under the conditions as shown in Table 1. The mixture was then filtered, and the filtrate was refrigerated prior to protein analysis. The residue was rinsed three times with the Sorensen phosphate buffer solution (3 x 50 mL). The second filtrate was also kept prior to protein analysis. The immobilized enzyme was dried in desiccator at room temperature and preserved in refrigerator before used. After immobilization, specific unit activity of both enzymes was determined using the Bernfeld method as conducted by Milosavic et al (2007).

Hydrolysis trials: 30 mL of 0.1 M acetate buffer solution at pH 4.6 was poured into two 100 mL Erlenmeyer flasks. Each starch was put into every flask at concentration of 3 mg-starch/mL. Then 2,500 U (tapioca) or 5,000 U (sorghum) enzyme (free- and immobilized type) was added into the flasks. All flasks were placed inside a water bath shaker operating at temperature of 60-80°C for 8 hours at agitation speed of 120rpm. Samples were collected and analysed using DNSA method.

Analysis

Analyses were run on POBA, sodium silicate, MCF silica, immobilized enzyme, glucose, and enzyme content. X-ray Fluorescence (XRF) analysis was performed to assess SiO_2 content using a PANalytical Epsilon 3 XRF unit located in the Chemical Instrumentation Lab in Universitas Negeri Padang (West Sumatera, Indonesia). Data regarding S_{BET}, pore volume, cell diameter, and window diameter were acquired using a Quantachrome Nova 1200e, which is part of the Integrated Lab in UPN Veteran (Yogyakarta, Indonesia). Fourier Transform Infrared Spectroscopy (FTIR) spectra were obtained with a PerkinElmer Spectrum IR 10.6.1 instrument from the Integrated Lab Unit in Universitas Diponegoro (Central Java, Indonesia). Pierce™ BCA protein assay kit was employed to estimate protein content following the standard method provided by the manufacturer. Hydrolysis of starch was assessed by using the DNSA (dinitrosalicylic acid) method. Enzyme contents and glucose samples were analyzed using a Thermo Scientific Genesys 10s UV-VIS spectrometer.

RESULTS AND DISCUSSION

SiO_2 content

Table 2 compares content of silica in raw and pretreated POBA. Percentage of silica increased from 20.593% (w/w) to 52.838% (w/w) following the pretreatment process of raw POBA with dilute sulphuric acid. Several compounds, namely: sulfur trioxide (SO_3) and potassium oxide (K_2O), reacted easily with H_2O to produce products dissolved in water directly. Some components dissolved in H_2O either slightly or highly. An important reduction was observed on ferric oxide (Fe_2O_3). Its content decreased highly after mixed with dilute sulphuric acid, but its percentage was considered still high after the pretreatment process. In the process, aluminium oxide (Al_2O_3) was considered not to react with H_2SO_4 as its percentage value was still high after the process. Because ferric oxide is more reactive than Al_2O_3, the sulphuric acid content would mainly react with the ferric oxide. As the experiment did not vary the sulphuric acid concentration, leaving impact of the acid on reduction of the POBA contaminants could not be known. The number of Fe_2O_3 and Al_2O_3 were considered still quite high after the process that required a further research optimisation. Stoichiometrically, quantity of H_2SO_4 required to convert 100% moles of Fe_2O_3 and Al_2O_3 to form soluble products, as shown in the equation (1) and (2), was around 22 mL that must be proved by an advanced experiment.

$$Fe_2O_{3(s)} + 3H_2SO_{4(aq)} \rightarrow Fe_2(SO_4)_{3(aq)} + 3H_2O_{(l)} \quad (1)$$

$$Al_2O_{3(s)} + 3H_2SO_{4(aq)} \rightarrow Al_2(SO_4)_{3(aq)} + 3H_2O_{(l)} \quad (2)$$

The obtained SiO_2 value in the raw POBA was consistent with the earlier findings. Bukit et al. (2022) reported the SiO_2 content of 27.3% (w/w) following their analysis of raw POBA from the North Sumatera region. Putri et al. (2025) recorded relatively high the SiO_2 percentage i.e. 38% (w/w) for the raw POBA originated from West Borneo. However, higher SiO_2 levels were found on the raw POBA from Malaysia and Thailand region, where the SiO_2 contents ranged from 40.60% to 65.3% (w/w) (Zarina et al., 2013; Tangchirapat et al., 2007; Tangchirapat et al., 2009).

Following the pretreatment of POBA, the pretreated residue was mixed with sodium hydroxide

Table 2. Major oxide compounds in POBA

Compound	Concentration (% w/w)		Solubility in water	Remark
	Raw	Pretreated		
Fe_2O_3	40.152	17.219	Insoluble	Forming $Fe_2(SO_4)_3$
SiO_2	20.593	52.838	Insoluble	No reaction
CaO	13.948	4.571	Slightly soluble	Forming $Ca(OH)_2$
Al_2O_3	11.986	14.958	Insoluble	Forming H_2SO_4
P_2O_5	3.842	2.872	Highly soluble	No reaction
SO_3	2.418	0.000	React with H_2O	Forming H_2SO_4
TiO_2	2.525	1.994	Insoluble	No reaction
K_2O	2.058	1.673	Soluble	Forming K_2SO_4

solution to transform the primary target, the SiO_2, into the sodium silicate solution. The reaction is as follows: (Sitohang et al., 2024; Kow et al., 2015):

$$SiO_{2(s)} + 2NaOH_{(aq)} \rightarrow Na_2SiO_{3(aq)} + H_2O_{(l)} \quad (3)$$

From this reaction, it is known that the quantity of SiO_2 that reacted with NaOH depended upon concentration of sodium hydroxide present in the mixture. The obtained stoichiometric calculation indicated that the quantity of NaOH compound used in the experiment was enough to react with the SiO_2 content.

The composition of the pretreated POBA after its reaction with the sodium hydroxide solution is presented in Table 3. According to XRF analysis, concentration of NaOH influenced formation of sodium silicate. The SiO_2 content in the filtrate solution increased from 76.434% (w/w) to 81.638% (w/w) as the NaOH concentration was increased from 40 mL to 60 mL. These finding suggested that a high portion of SiO_2 reacted with NaOH. However, high NaOH concentration also led to the increase of aluminum oxide level dissolved in the water glass solution as NaOH could function as a strong base activator in the mixture. It was undesirable as a high Al_2O_3 level would hinder development of the MCF silica structure. Hence, reduction of Al_2O_3 highly in the acidification step was important.

Several comparable routes had been established. Sitohang et al. (2024) reacted the pretreated POBA with 6 M NaOH to create mesoporous silica, which was utilized to support methyl ester sulfonate. In contrast, Adha and Warsiki (2023) dissolved the POBA-derived SiO_2 in various concentrations of NaOH solution to obtain sodium silicate, which subsequently was employed as an adsorbent of moisture. Unfortunately, neither of both studies disclosed the SiO_2 content in the waterglass solution.

Synthesis of POBA-derived MCF silica

During synthesis of the MCF silica, the NaOH volume was varied in range of 40-60 mL to determine the role of Na_2SiO_3 in formation of the silica. Results of the Brunauer–Emmett–Teller (BET) analysis are presented in Tabel 4. In general, the increase of NaOH volume resulted in reduction of the MCF silica surface area, pore volume, cell and window diameter, with particularly a significant decrease was observed in the window diameter. In term of S_{BET}, the MCF silica-40 gave the highest surface area. All silica products showed similar pore volume and cell diameter, however, the window diameter tended to decrease highly when the NaOH volume was high. Based-on the Brunauer–Emmett–Teller characteristics, the MCF silica@NaOH-40 showed the most optimal characteristics with specific surface area of 551.1 m^2/g, specific pore volume of 1.592 cm^3/g, cell pore diameter of 167.4 Å, and window pore diameter of 126.9 Å. This largest window pore diameter indicated better pore accessibility compared to other silicas, so that more optimal mesopore structure was formed. Hence, NaOH plays a significant role in helping to determine formation of pore structure of the MCF silica.

In this study, NaOH functioned as a chemical compound that reacted with 9 grams SiO_2 (solid phase) to produce sodium silicate (liquid phase), which then was converted into the MCF silica. As described in Table 4, 60 mL of 3 M NaOH tended to dissolve more SiO_2, but it also increased dissolution of aluminum oxide that could interfere formation of the MCF silica structure. Therefore, volume of NaOH 40 mL and 50 mL was better to be used because the NaOH solution dissolves less aluminum oxide. From BET analysis, it could be known that these NaOH volumes produced similar pore volume, cell and window diameter,

Table 3. Composition of the sodium silicate filtrate

Compound	Final concentration (% w/w)			Remark
	NaOH 40 mL	NaOH 50 mL	NaOH 60 mL	
SiO_2	76.434	80.626	81.638	React with NaOH
P_2O_5	6.952	1.782	5.061	Dissolve in H_2O
CaO	2.258	0.278	1.594	Dissolve in H_2O
Al_2O_3	2.469	2.002	10.315	React with NaOH
K_2O	1.566	0.503	0.671	Dissolve in H_2O
TiO_2	0.002	0.021	0.032	React with NaOH
Fe_2O_3	0.149	0.369	0.584	Not dissolve

Table 4. Characteristics of MCF silica at different NaOH volume

Compound	S_{BET} (m^2/g)	V_{pore} (cm^3/g)	d_{cell} (Å)	d_{window} (Å)	Remark
MCF silica@NaOH-40	551.1	1.592	167.4	126.9	P123: 5 g KCl: 5 g AcOH: 2.2 mL
MCF silica@NaOH-50	437.2	1.581	167.9	126.6	
MCF silica@NaOH-60	524.8	1.429	167.3	97.84	
MCF silica@P123-4 g	473.0	1.697	167.6	127.1	NaOH: 40 mL KCl: 5 g AcOH: 2.2 mL
MCF silica@P123-5 g	551.1	1.592	167.4	126.9	
MCF silica@P123-6 g	517.0	2.008	167.4	97.83	
MCF silica@AcOH-2.2	551.1	1.592	167.4	126.9	NaOH: 40 mL P123: 5 g KCl: 5 g
MCF silica@AcOH-3.3	589.8	2.004	167.1	97.86	
MCF silica@AcOH-4.4	739.0	2.046	167.1	97.76	
MCF silica@KCl-5 g	739.0	2.046	167.1	97.76	P123: 5 g AcOH: 4.4 mL NaOH: 40 mL
MCF silica@KCl-7.5 g	508.2	0.993	55.63	79.3	
MCF silica@KCl-10 g	459.8	1.019	94.07	79.23	
MCF silica@KCl- 15 g	382.2	0.719	33.95	56.84	

except the surface area, so that the NaOH 40 mL was preferred. Besides this, the NaOH 50 mL gave larger iron oxide content than the NaOH 40 mL, but a slightly smaller Al_2O_3 content. High Fe_2O_3 content caused interference with formation of the MCF silica structure.

The use of NaOH to form waterglass compound gave quite similar results. Recent study conducted by Agustian and Hermida (2025) demonstrated the production of MCF silica from bagasse bottom ash (BBA), where 11 grams of BBA were transformed into sodium silicate using 50 mL of 3M NaOH and subjected to heating at 80°C for duration of four hours. In a related study, Sitohang et al (2024) synthesized the mesoporous silica from POBA by forming the sodium silicate with 6 M NaOH at temperature of 80°C for one hour. Previously, Porrang et al (2021) produced silica nanoparticles from rice husk by applying 7.04 mL of 1 M NaOH for every gram of rice husk, which was then heated at 80°C for one hour.

Synthesis of the MCF silica from POBA was continued by adjusting concentration of Pluronic® P123 within the range of 4-6 grams, while maintaining other parameters constant. Throughout the experiments, as shown in Table 5, there was a noticeable increase in both the surface area and volume of pore; however, the window diameter significantly decreased, while the cell diameter stayed the same. The highest surface area was achieved with the Pluronic® P123 amount of 5 g where the S_{BET}, V_{pore}, d_{cell}, and d_{window} were recorded as 551.1 m^2/g, 1.592 cm^3/g, 167.4 Å, and 126.9 Å, respectively. Pluronic® P123 functions as the structural template. Insufficient template leads to underdeveloped structure, whereas excessive amount of template can reduce the pore window diameter and compromise the stability of the pore structure.

In comparison to the earlier studies, quantity of the Pluronic P123 used in the mesoporous silica synthesis was not markedly different. Most experiments conducted on the laboratory scale consumed 4 grams of Pluronic P123 in the synthesis (Hermida and Agustian, 2025; Agustian and Hermida, 2019a,b; Hao et al., 2019; Agustian and Hermida, 2018; Luo et al., 2017; Hermida et al., 2013). However, Agudelo et al. (2020) supplied a lesser amount i.e. only 2.4 grams.

Following determination of the optimal concentration of sodium hydroxide and Pluronic P123, the subsequent factor adjusted in synthesis of the MCF silica was concentration of acetic acid. This is crucial as pH significantly influences rate of hydrolysis and condensation reaction of the silica precursors, thereby impacting development of mesoporous structures. Acetic acid substituted HCl, which is harmful to environment and typically used in the MCF silica synthesis (Agustian dan Hermida, 2025, 2024, 2018, 2019a,b). Volume of acetic acid was maintained around 2.2-4.4 mL, while all other parameters remained unchanged. Based-on BET characteristics, increasing acetic acid quantity improved both the specific surface area and pore volume, while concurrently causing reduction in the window diameter. The cell diameter, however, remained constant. The MCF silica product had the highest specific surface area of 739.0 m^2/g and specific pore volume of 2,046 cm^3/g, but it had the smallest window diameter

(97.76 Å). Variation in the amount of acetic acid resulted in changes on the pore structure formation, which in turn affected the specific surface area, pore volume, and pore size of the material. The effect of increasing acetic acid quantity helped accelerate the hydrolysis and condensation process of silica, resulting in a more developed mesopore structure with a larger surface area. Compared with the earlier finding, the optimal results obtained in these experiments exhibited the increased of surface area and pore volume, alongside with reduction of cell size, while the window size remained consistent. For example, Choi et al. (2015) supplied 2.2 mL of acetic acid in the synthesis of salt-derived MCF silica from commercial sodium silicate solution. They obtained surface area ranging from 309 to 453 m^2/g, pore volume between 1.28 and 1.56 cm^3/g, cell size varying from 23.6-32.4 nm, and window size of 5.76-13.7 nm.

The last experimental impact was observed on KCl variation. The chemical was utilized to substitute mesitylene. Like TEOS, mesitylene is an imported substance in Indonesia, costly, and not readily accessible; therefore, finding another suitable compound is deemed essential. The salt contributed to formation of the mesoporous structure by influencing interaction between silica precursors and Pluronic P123, thereby affecting development of pore structure of the MCF silica. In the experiments, the amount of KCl was varied in the range of 5-15 grams. All experimental results showed that high KCl quantity led to reduction of the surface area, pore volume, cell and window diameter. The best MCF silica was developed by the KCl quantity of 5 grams where the S_{BET}, V_{pore}, d_{cell}, and d_{window} were 739.0 m^2/g, 2.046 cm^3/g, 167.1 Å and 97.76 Å, respectively. This superior MCF silica enhanced capacity for adsorption processes, catalysts, or other molecular interaction. Moreover, the high pore volume indicated that the MCF silica possessed substantial internal voids, thereby enabling it to hold a greater quantity of substances. These could be attributed by the function of KCl as a charge-regulating agent or electrolyte during the MCF silica synthesis. Its concentration could compromise stability of pore template, resulting in a denser and less porous silica structure.

Quantity of KCl used in these experiments was comparable to that used in the prior studies. Agustian and Hermida (2025) employed 10 grams of KCl to synthesize the MCF silica from the BBA. Choi et al. (2015) observed the effect of KCl in the range of 1-20 grams in the production of MCF silica from sodium silicate, where the amount of 3-10 grams yielded the best superior characteristics of the MCF silica.

In comparison to the mesitylene-derived MCF silica, the surface area and volume of pore of the MCF silica synthesized using both chemical agents (KCl or mesitylene) showed no significant differences. Agudelo et al. (2022), who synthesized the MCF silica from TEOS and mesitylene, reported the surface area of 797.6 m^2/g and volume of pore of 2.17 cm^3/g. Several recent studies indicated S_{BET} values of less than 500 m^2/g, although the pore volume of the resulting MCF silica remained consistent at approximately 2.1 cm^3/g (Hermida et al. 2013; Agustian and Hermida 2018, 2019a,b,c; Luo et al. 2017). Nevertheless, the products derived by mesitylene generally displayed larger cell and window diameters. Specifically, these products typically exhibited the cell and window diameters ranging from 219.5 to 296 Å and 100 to 150 Å, respectively (Hermida et al. 2013; Agustian and Hermida 2018, 2019a,b,c; Luo et al. 2017; Agudelo et al. 2022), while the KCl-derived MCF silica had the cell and window diameter of less than 200 Å and 100 Å, respectively.

MCF silica pore sizes

The window and cell pore size distribution of the MCF silica obtained by varying the experimental factors, are shown in Figure 2. Based-on the factor optimization as shown in Table 4 and the Barrett-Joyner-Halenda (BJH) adsorption-desorption analysis, it is clear that the pore size characteristics of the optimal MCF silica product—derived from variation of NaOH solution and Pluronic P123—were same as shown in Figure 2-left. Similarly, the MCF silica product resulting from variation of acetic acid exhibited the pore size characteristics that were identical to those obtained from variation of KCl (Figure 2-right). Two peaks were observed in each graph, indicating that the synthesis process successfully formed the MCF silica pore structure consisting of both the cell and window pores.

Most of the cell and window pore diameter fall within the mesoporous pore size range, typically 2–50 nm. During the NaOH and Pluronic P123 variation, the pore diameter for the cell and window were found in the range of 34–521 Å (3.4–52.1 nm) and 31–297 Å (3.1–29.7 nm), respectively, as described in Figure 2-left. The optimal cell and window pore diameter were

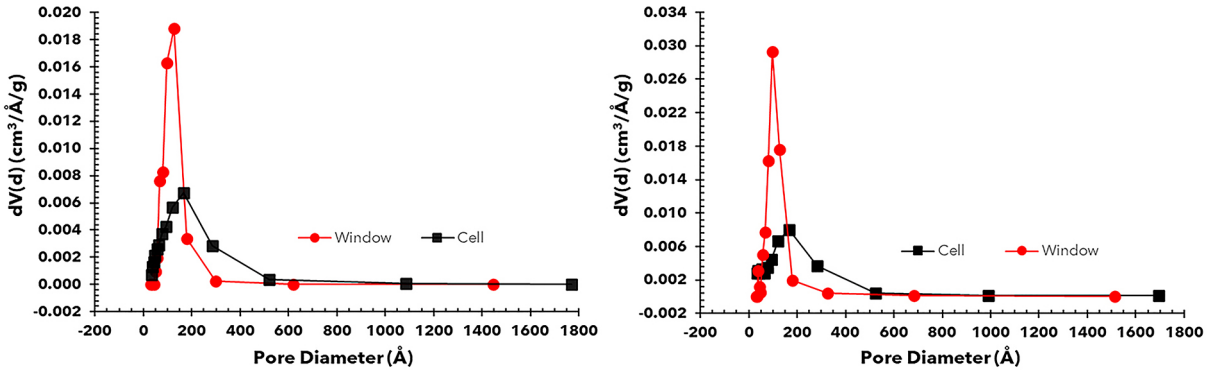

Figure 2. The optimal cell and window pore size distribution (left: variation of NaOH and Pluronic P123; right: variation of acetic acid and KCl)

determined to be 167.405 Å and 126.919 Å, respectively. Figure 2-right further confirmed that the cell pore diameter during the acetic acid variation were consistent with those observed during the NaOH and Pluronic P123 variation, specifically ranging from 34 to 521 Å (3.4–52.1 nm), but the window pore diameters were recorded within the range of 30–326.5 Å (3.03–32.65 nm). Under these factorial variations, the optimal pore diameter for the cell and window were found to be 167.114 Å and 97.757 Å, respectively. All optimal pore sizes were located within the established pore size distribution range. Additionally, both figures illustrated the changes that occurred when the process factors were modified. The range of cell diameters appeared to remain stable when the synthesis factors were altered; however, the diameter range for the window and peak shifted as the synthesis operating factors were increased.

Figure 3 displays the hysteresis loops resulting from variation of the synthesis factors. Both curves exhibit volume changes at high relative pressure region (P/Po>>). They reflected a type IV hysteresis pattern, characterized by a hysteresis loop at intermediate to high (P/Po) values. Barton et al. (1999) described that a type IV hysteresis indicated a mesoporous material with pore sizes ranging from 2 to 50 nm. Presence of the hysteresis loop signified capillary condensation within the material pores during the nitrogen adsorption-desorption process occurring in the mesoporous structure. Furthermore, the distinct hysteresis loop indicated that the formed pores were well-interconnected, thereby facilitating molecular diffusion into the material.

The nitrogen adsorption-desorption isotherm curve for the optimal MCF silica synthesized under NaOH and Pluronic P123 variation (Figure 3-left) informs a significant increase in the volume of adsorbed nitrogen within the (P/P_0) range of 0.696–0.98. The sharp increase indicated presence of a large pore volume and a well-interconnected pore system. These results aligned with the BET data showing that the optimal MCF silica product possessed the specific surface area of 551.10 m^2/g and pore volume of

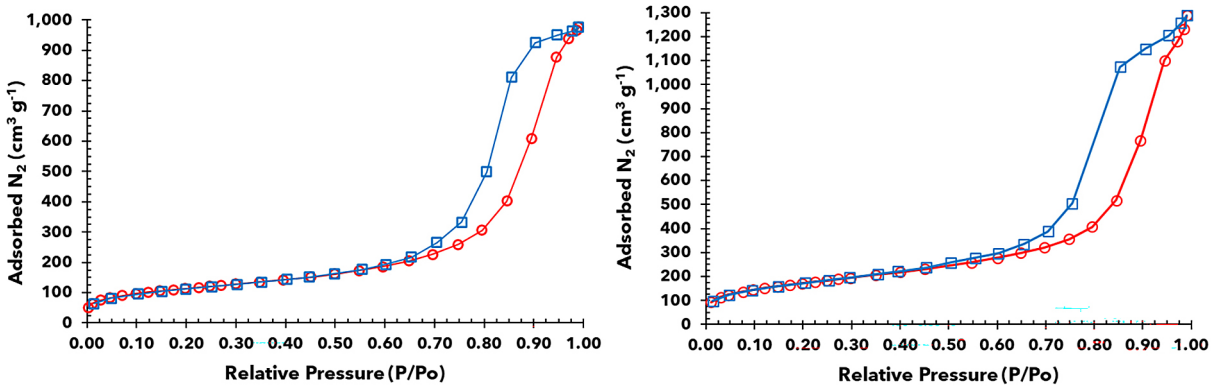

Figure 3. Isotherm adsorption-desorption nitrogen of POBA-derived MCF silica (left: NaOH & Pluronic P123 variation; right: acetic acid & KCl variation)

1.592 cm³/g. Such characteristics demonstrated that the raw material variation successfully produced a well-developed mesoporous structure that facilitated formation of an optimal MCF silica product.

A similar pattern is observed on the nitrogen adsorption-desorption isotherm curve for the MCF silica synthesized from different acetic acid and KCl quantity (Figure 3-right). The curve shows a sharp increase in the nitrogen adsorption volume within the (P/P_0) range of 0.696–0.991. This rise indicated occurrence of capillary condensation within the formed mesopores. The high nitrogen adsorption volume—approaching a value of 1—indicated a significant adsorption capacity and large pore volume. This high adsorption volume was consistent with the BET results showing the specific surface area of 739 m²/g and a pore volume of 2.046 cm³/g.

Based-on the BET analysis, it could be concluded that variations of the operating conditions in synthesis of the MCF silica reached an optimal point regarding formation of the mesoporous structure. The optimal synthesis conditions were obtained at a combination of 40 mL NaOH, 5 g Pluronic P123, 4.4 mL CH_3COOH, and 5 g KCl. This combination yielded the MCF silica characterized by homogeneous morphology, high surface area, and optimal pore accessibility.

Immobilization of enzyme

Glucoamylase was used as a model enzyme for immobilization on the POBA-derived MCF silica, as the enzyme is widely employed in starch saccharification processes to produce reducing sugars, which are used to generate ethanol, glucose, and other products. Immobilization of glucoamylase on the support matrix was made by varying the process factors. Temperature, Sorensen phosphate buffer pH, enzyme concentration, and agitation speed were varied during the immobilization process. Effects of the factors are shown in Figure 4.

Temperature plays a vital role in immobilization of enzyme, as it affects stability of the enzyme's structure and its interactions. In the experiments, temperature of immobilization was adjusted within the range of 30-40°C, while all other conditions remained unchanged. The optimal enzyme immobilization occurred at temperature of 35°C, yielding an immobilization process efficiency of 70.98% (w/v). Deviation from this temperature, either higher or lower, resulted in a decrease in efficiency; however, variation in efficiency was minimal, ranging from 1.5% to 2.1% (w/v). Therefore, the temperature range of 30-40°C was considered appropriate for immobilization of free glucoamylase on the POBA-derived

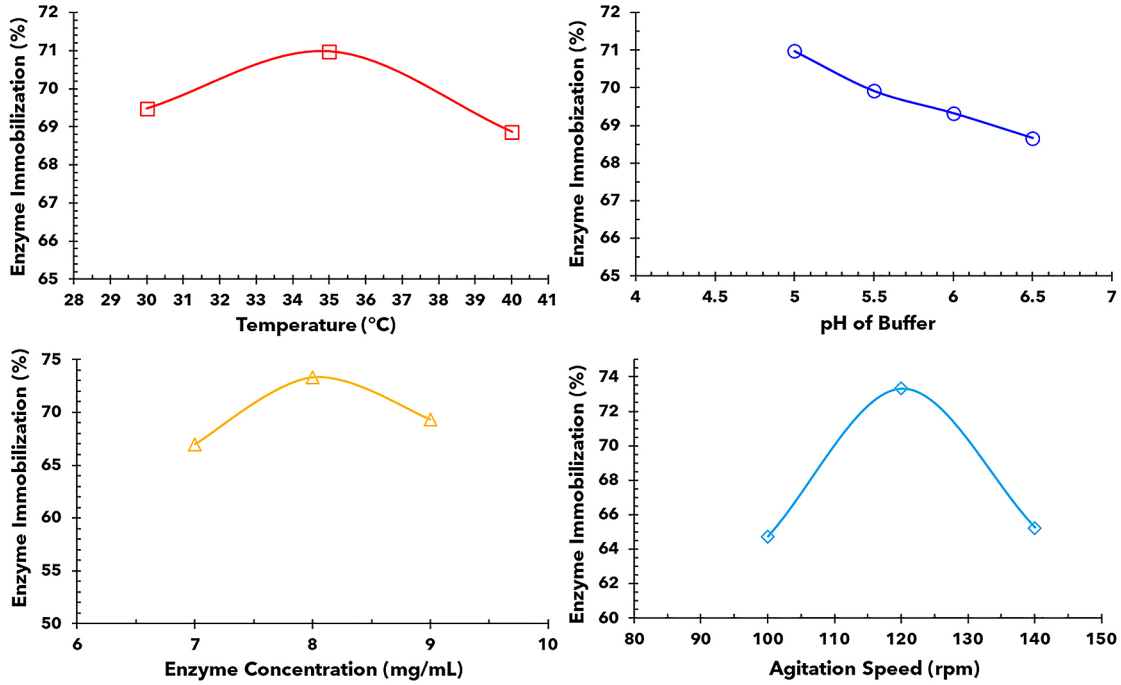

Figure 4. Effects of factors on the immobilization process (top-left: buffer pH 6, 9 mg/mL enzyme, 120 rpm; top-right: 35°C, 9 mg/mL enzyme, 120 rpm; bottom-left: 35°C, buffer pH 6, 120 rpm; bottom-right: 35°C, buffer pH 6, 8 mg/mL enzyme)

MCF silica matrix. These results align with the literature stating that the immobilized glucoamylase exhibit good activity and stability at temperatures of 30–40°C (Agustian et al., 2025). At temperature of 30°C, movement of enzyme molecules is generally slower compared to that at temperature of 35°C. As a result, the enzyme ability to enter the MCF silica pores and its interaction with the silica surfaces did not occur at an optimal level, leading to a lower amount of successfully immobilized enzyme. An increase in the immobilization temperature beyond 35°C resulted in a decrease in the amount of immobilized enzyme, as the higher temperatures enhance the mobility of enzyme molecules, thus making the bonds established between the enzyme and MCF silica surface less stable (Mateo et al., 2007).

The next step was to observe the effect of Sorensen phosphate buffer pH. A 100 mM buffer was used, with pH levels varied in the range of 5.0-6.5. Other operational factors were constant. The immobilized enzyme efficiencies tended to decrease as the pH rose. The optimal result was found at pH of 5.0 where the efficiency was 70.98% (w/v). Decreasing the buffer pH reduced the immobilization efficiencies. At pH of 6.5, performance of the process reduced to 68.66%, which was 2.32% lower than the optimal result. However, the difference within the pH range of 5.0-6.0 was small—only about 1.06-1.65%—indicating that this pH range was considered quite suitable for the immobilization of the glucoamylase enzyme. pH of 6.0 was selected to be the optimal condition; it not only achieves a sufficiently high percentage of immobilization, but also provides a near-neutral pH, which is more feasible for implementation on industrial scales and leads to less complex waste processing. Although acidic conditions can enhance the interaction between the enzyme and silica surface, excessively acidic pH levels may jeopardize the stability of the enzyme structure. Excessively acidic conditions can lead to changes in the structural configuration of the enzyme or result in protein denaturation, consequently diminishing enzymatic activity. pH variations that deviate far from the optimal range can interfere with the bonds that uphold the enzyme structure, resulting in decreased enzyme stability.

Impact of free enzyme concentration on the immobilization process was examined within the range of 7-9 mg/mL. As illustrated in Figure 3, variation in the enzyme concentration influenced the immobilization efficiency. The highest efficiency was 73.33% (w/v), achieved at the free glucoamylase concentration of 8 mg/mL. Beyond this optimal concentration, the efficiency declined to 66.96% (w/v) at 7 mg/mL and to 69.33% at 9 mg/mL. An increase in the free enzyme concentration from 7 mg/mL to 8 mg/mL resulted in a greater number of enzymes adhering to surfaces of the POBA-derived MCF silica, as more binding sites were available. However, when the free enzyme concentration was raised to 9 mg/mL, the immobilization efficiency decreased. This reduction occurred because, although the number of free enzymes attached to the support surfaces had reached the optimal level, many free enzymes remained dissolved in the buffer solution, which negatively impacted the efficiency of enzyme immobilization.

The final factor was speed of agitation. It was determined that the speed influences the immobilization efficiencies. At the agitation speed of 100 rpm, efficiency of 64.739% was obtained. The optimal efficiency reached 73.33% at the speed of 120 rpm. Increasing the agitation speed from 100 rpm to 120 rpm improved the interaction between the enzyme and support surfaces. However, speeds exceeding the optimal value tended to decrease the immobilization efficiency. The reduction occurred because excessive stirring intensity led to increased inter-particle collisions, causing some enzymes that were already bound to the silica surface to detach and re-enter the solution. Additionally, the immobilization method used was adsorption, which is characterized by relatively weak bonds between the enzyme and the matrix, making detachment more likely under high-speed conditions. The result indicated that the optimum agitation speed for glucoamylase immobilization was 120 rpm. This finding aligns with the previous study that reported the immobilization efficiency on the MCF silica reaches its optimum value at speed of 120 rpm (Agustian and Hermida, 2025).

Immobilization of free enzyme on the MCF silica matrix was proved by BET and FTIR analysis. The BET results indicated that the matrix surface area decreased from 879.54 m^2/g to 510.80 m^2/g after the immobilization process. Furthermore, the pore volume of the matrix reduced from 1.863 cm^3/g to 1.115 cm^3/g. Analysis of FTIR is shown in Figure 5. Three main differences on both spectra were observed as marked in the red boxes. Large vibrations were found at 3,384 cm^{-1} (immobilized enzyme) and 3,382 cm^{-1} (MCF silica), however the immobilized glucoamylase showed a bigger spectrum than the matrix. The peak related

to the hydroxyl group, primary amide group, secondary amine group, and Si-OH stretch (Kannan and Jasra, 2009; Actim, 2014; Zhang et al., 2008; Jin et al., 2011). For carboxylic acids, the O-H band is very broad and centred around 3,400 cm^{-1} where the NH-bands are usually sharper than O-H bands (Derrick et al., 1999). The second difference was found at the vibration peaks of 1,636 cm^{-1} (immobilized enzyme) and 1,633 cm^{-1} (the matrix). The vibrations were low, but the immobilized enzyme showed a slightly higher spectrum than the support. Theoretically, these spectra occurred in the carbon double bond region, which associated with the functional groups of C=C stretching, primary amine, secondary amine, amide, and organic nitrates (Kannan and Jasra, 2009; Actim, 2014; Zhang et al., 2008; Jin et al., 2011). The final difference was observed at the peak of 684 cm^{-1} where the immobilized enzyme showed a small vibration, which was not found on the support matrix. The possible compounds, which probably exist around this vibration, are halogen and aromatic molecules (Lambert et al., 1998). As glucoamylase consists of amino acids having the amino groups ($-NH_2$), carboxyl groups (-COOH) and aromatic molecules, the spectrum of immobilized enzyme indicated the presence of enzyme of the matrix.

Tapioca and sorghum starch hydrolysis

Prior to the hydrolysis trials, it was essential to determine specific activity of the free and immobilized glucoamylase. They were evaluated to determine enzyme activity unit (U), which indicate ability of the enzyme to hydrolyze starches into reducing sugars. Evaluation was performed following the method established by Milosavic et al. (2007), which employed glucoamylase in both states, free and immobilized. The activity assay was performed using a soluble starch, with each type of enzyme evaluated in duplicate. Samples were gathered every 5 minutes throughout a 30-minute time to quantify the reducing sugar.

The average specific activity of free and immobilized glucoamylase was 10,788.354 U/g and 5,811.154 U/g, immobilized, respectively. The specific activity of free glucoamylase surpassed that of the immobilized variant. The higher activity of the free enzyme was ascribed to its unobstructed condition, enabling its active sites to engage directly with the substrate without interference. Consequently, this led to a more efficient reaction, yielding higher activity values. In contrast, reduction in the enzyme activity observed after the immobilization process could be attributed to the conformational changes in glucoamylase that occurred during the process, which made the enzyme active sites less effective for the substrate bindings. Additionally, the attachment of enzyme to the support might obstruct diffusion of substrate towards the active sites, thereby reducing the enzyme activity. The specific activity of the glucoamylase immobilized onto the POBA-derived MCF silica matrix was relatively higher than the previous results. Agustian and Hermida (2018, 2019a,b,c) obtained the specific enzyme activity of 1.856.78 U/g for glucoamylase immobilized onto the TEOS-based MCF silica.

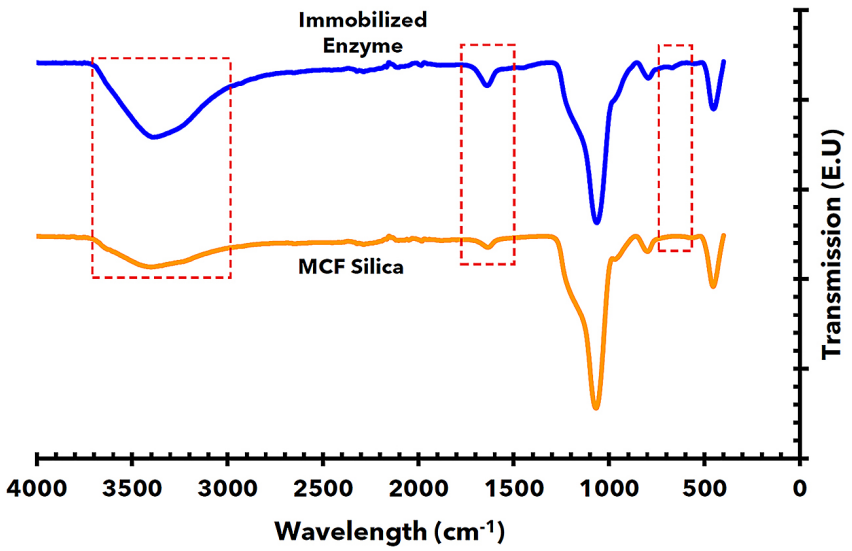

Figure 5. Spectrum of the MCF silica and immobilized enzyme

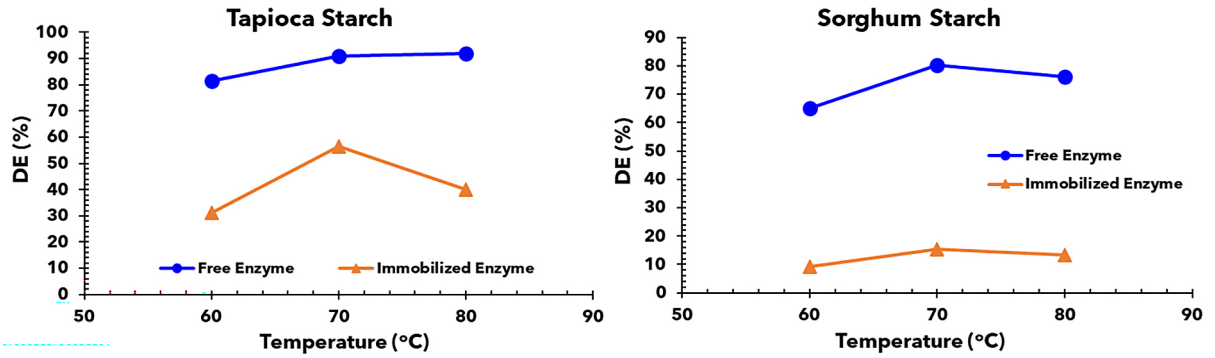

Figure 6. Hydrolysis of tapioca and sorghum starch using free and immobilized glucoamylase at different temperatures

Observation on tapioca and sorghum starch hydrolysis was performed to reveal capability of the immobilized glucoamylase operated under at some temperatures(60-80°C). The result is shown in Figure 6.

During the hydrolysis processes, the temperature factor was found to influence the processes. The immobilized glucoamylases were found to have lower DE values than free enzymes. The immobilized enzymes produced DE values of 31.3-56.61% (w/w) (tapioca) and 9.25-15.37% (w/w) (sorghum), which peaked at temperature of 70°C. The free glucoamylases had the optimum DE value of 92.01% (w/w) for conversion of tapioca starch obtained at temperature of 80°C), while the DE value as high as 80.18% (w/w) was obtained in conversion of sorghum starch at temperature of 70°C. Free glucoamylase was more effective in hydrolysing the starches as more active sites were available to interact with the substrate molecules, while the immobilized glucoamylase had lesser active sites for the tapioca molecules due to the immobilization process that changed or blocked some enzyme active sites. These results indicated that increasing temperature led to the increase of DE. Nelson and Cox (2005) stated that enzyme activity generally rises with increasing temperature until the optimum temperature is reached. However, excessively high temperatures—specifically 80°C—cause protein denaturation, alter enzyme's structure and reduce enzyme capability (Hermida et al., 2019).

The optimum hydrolysis temperature using the immobilized enzyme aligned with the previous result conducted by Agustian and Hermida (2019a,b.c) who reported the optimum temperature range for the starch hydrolysis using glucoamylase immobilized on the silica MCF matrix was 60-70°C, with the optimum temperature of 70°C. The result indicated that the immobilized glucoamylase retained its activity and stability at relatively high temperatures, up to the optimum level.

CONCLUSIONS

Pretreatment of POBA using diluted H_2SO_4 removed impurity oxides, so that content of SiO_2 increased from 20.593% (w/w) to 52.838% (w/w). Reaction between the pretreated POBA with sodium hydroxide solution also increased the SiO_2 content to as high as 81.638% (w/w). Synthesis of MCF silica from POBA was conducted successfully by varying concentration of NaOH, Pluronic® P123, acetic acid, and KCl. The optimum chemical concentrations were determined to be 40 mL of NaOH, 5 grams of Pluronic® P123, 4.4 mL of acetic acid, and 5 grams of KCl. The optimum values yielded the MCF silica having specific surface area of 738.976 m^2/g, volume of pore of 2.046 cm^3/g, pore cell diameter of 167.114 Å, and pore window diameter of 97.757 Å. Concentration of NaOH and KCl showed adverse effects on formation of the product, as the elevated concentrations diminished the MCF silica surface area, pore volume, and both cell and window diameters. Increasing concentration of Pluronic P123 and acetic acid enhanced the surface area and volume of pore of the MCF silica, but they substantially reduced the window diameter, while the cell diameter remained the same. Glucoamylase immobilization was conducted by varying temperature, pH of buffer solution, initial concentration of free enzyme, and stirring speed of the process to give the maximum efficiency of 73.33% at temperature of 35°C, buffer pH of 6.0, initial free glucoamylase concentration of 8% (240 mg/30 mL), and stirring speed of 120 rpm.

Capability of immobilized glucoamylase were observed via starch hydrolysis by varying the process temperature to give DE values as high as of 56.61% (w/w) (tapioca substrate) and 15.37% (w/w) (sorghum substrate) obtained at the operational temperature of 70°C.

Acknowledgements

All authors wish to express their appreciation to Directorate General of Research and Development, Ministry of Higher Education, Science, and Technology Republic of Indonesia, for providing a financial support in 2025 through Fundamental Research Grant No. 512/UN26.21/PN/2025.

REFERENCES

1. Asyri, F., Hafni, K.N., & Simamora, A.H. (2015). Effect of oil palm biomass combustion ash waste on the physical and mechanical properties of high-impact polystyrene. *Jurnal Teknik Kimia USU*, 04(3), 23-28 (in Indonesian). https://talenta.usu.ac.id/jtk/article/view/1477/957
2. Bagus, H. (2023). Analysis of the use of palm oil mill boiler ash as an additive on concrete compressive strength. (in Indonesian). Thesis. Department of Civil Engineering. University of Medan Area.
3. Yoescha S.R. (2007). Utilization of oil palm ash as an additive in concrete mixtures. (in Indonesian). Thesis. Department of Civil Engineering. University of Andalas.
4. Putri, R.C., Silalahi, I.H., Zaharah, T.A., & Widiyantoro, A. (2025). Study on the utilization of palm oil fuel ash and carbide waste as a concrete mixture. *Positron*, 15(02), 143-156. https://jurnal.untan.ac.id/index.php/jpositron/article/view/88882/pdf
5. Bukit, B.F., Frida, E., Humaidi, S., Sinuhaji P., & Bukit, N. (2022). Optimization of palm oil boiler ash biomass waste as a source of silica with various preparation methods. *Journal of Ecological Engineering*, 23(8), 193-199. https://doi.org/10.12911/22998993/150694
6. Piumetti, M., Bonelli, B., Massiani, P., Dzwigaj, S., Rossetti, I., Casale, S., Armandi, M., Thomas, C., & Garrone, E. (2012). Effect of vanadium dispersion and of support properties on the catalytic activity of V-containing silicas. *Catalysis Today*, 179, 140-148. https://doi.org/10.1016/j.cattod.2011.06.028
7. Chunguang, L., Changxi, M., Yingying, N., Yinghong, Y., Songyuan, G., Weimin, Y., Weiming, H., & Zi, G. (2010). Ethylbenzene dehydrogenation in the presence of CO_2 over MCF-supported vanadium oxide catalysts. *Chinese Journal of Catalysis*, 31, 993-998. https://doi.org/10.1016/S1872-2067(10)60099-X
8. Ginting, Y.C., Hermida, L., Agustian, J., Rugayah, & Taufiqurrahman, R. (2018). Testing the application of various types of slow-release urea fertilizers on growth of Pakcoy (*Brassica rapa chinensis*). *Prosiding Semnas SINTA FT UNILA*, 1, 35-41. (in Indonesian). https://www.researchgate.net/publication/341541534_Uji_Aplikasi_Berbagai_Jenis_Pupuk_Urea_Lepas_Lambat_Terhadap_Pertumbuhan_Tanaman_Pakcoy_Brassica_rapa_chinensis
9. Rugayah, Hermida, L., Ginting, Y.C., & Agustian, J. (2019). Application test of various types of slow-release urea fertilizer on growth of Kailan plant (*Brassica oleraceae* L.). *Prosiding Semnas SINTA FT UNILA*, 1, 42-48. (in Indonesian). https://www.researchgate.net/publication/341541719_Uji_Aplikasi_Berbagai_Jenis_Pupuk_Urea_Lepas_Lambat_Slow_Release_Urea_Terhadap_Pertumbuhan_Tanaman_Kailan_Brassica_oleraceae_L
10. Sriagung, D., Rugayah, Ginting, Y.C., & Hermida, L. (2021). Evaluation of several types of slow-release nitrogen fertilizers on cauliflower (*Brassica oleracea* var. *botrytis* L.) plant receiving NPK basal fertilizer. *Agrotek Tropika*, 9(3), 481-487. (in Indonesian). https://doi.org/10.23960/jat.v9i3.5309
11. Hermida, L., Abdullah, A.Z., & Mohamed, A.R. (2013a). Synthesis and characterization of mesostructured cellular foam (MCF) silica loaded with nickel nanoparticles as a novel catalyst. *Materials Sciences and Applications*, 4, 52-62. http://dx.doi.org/10.4236/msa.2013.41007
12. Hermida, L., Abdullah, A.Z., & Mohamed, A.R. (2013b). Nickel functionalized mesostructured cellular foam (MCF) silica as a catalyst for solventless deoxygenation of palmitic acid to produce diesel-like hydrocarbons. In Materials and processes for energy: communicating current research and technological development. Mendez-Vilas, A. (Ed),. Formatex Research Center C/ Zurbarán 1, 2º, Oficina 1 06002. Badajoz Spain. https://www.researchgate.net/publication/272482676_Nickel_functionalized_mesostructured_cellular_foam_MCF_silica_as_a_catalyst_for_solventless_deoxygenation_of_palmitic_acid_to_produce_diesel-like_hydrocarbons#fullTextFileContent
13. Agustian, J., & Hermida, L. (2024). Magnetic mesoporous cellular foam silica to support free amylolytic enzymes: Synthesis and amylases immobilization. *AIP Conference Proceedings*, 2891, 090020. AIP Publishings. https://doi.org/10.1063/5.0203288
14. Agustian, J., & Hermida, L. (2019a) Capability of immobilised glucoamylase on mesostructured cellular foam silica to hydrolyse tapioca starch. *IOP Conference Series: Material Science and Engineering*, 509, 012058. Institute

of Physics Publishing. https://iopscience.iop.org/article/10.1088/1757-899X/509/1/012058

15. Agustian J. and Hermida L. (2019b). Mesostructured cellular foam MCF- (9.2T-3D) silica as support for free α-amylase in liquefaction of tapioca starch, *IOP Conference Series: Material Science and Engineering*, 509, 012059. Institute of Physics Publishing. https://iopscience.iop.org/article/10.1088/1757-899X/509/1/012059
16. Agustian, J., & Hermida, L. (2019c). The optimised statistical model for enzymatic hydrolysis of tapioca by glucoamylase immobilised on mesostructured cellular foam silica. *Bulletin of Chemical Reaction Engineering & Catalysis*, 14, 380-390. https://doi.org/10.9767/bcrec.14.2.3078.380-390
17. Agustian, J., & Hermida, L. (2018). Saccharification kinetics at optimized conditions of tapioca by glucoamylase immobilised on mesostructured cellular foam silica. *Eurasian Chemico Technological Journal*, 20(4), 311-318. https://doi.org/10.18321/ectj764
18. Hermida, L., Amani, H., Abdullah, A.Z., & Mohamed, A.R. (2016). Deoxygenation of palmitic acid to produce diesel-like hydrocarbons over nickel incorporated cellular foam catalyst: a kinetic study. *Journal of Advance Chemical Engineering*, 6, 1-8. https://www.researchgate.net/publication/299949623_Deoxygenation_of_Palmitic_Acid_to_Produce_Diesel-like_Hydrocarbons_over_Nickel_Incorporated_Cellular_Foam_Catalyst_A_Kinetic_Study
19. Hermida, L., Agustian, J., Abdullah, A.Z., & Mohamed, A.R. (2019). Review of large-pore mesostructured cellular foam (MCF) silica and its applications. *Open Chemistry*, 17(1), 1000-1016. https://doi.org/10.1515/chem-2019-0107
20. Agudelo, N.A., Escobar, S., Tejada, J.C., & López, B.L. (2020). Understanding of the formation of mesocellular-like silica foam particles of nano size and its chemical surface to immobilization of *Thermomyces lanuginosus* lipase. *Microporous and Mesoporous Materials*, 294, 109948. https://doi.org/10.1016/j.micromeso.2019.109948
21. Agudelo, N.A., Echeverri-Cuartas, C.E., & López, B.L. (2022). Composite membranes based on functionalized mesostructured cellular foam particles and sulfonated poly(ether sulfone) with potential application in fuel cells. *Membranes*, 12, 1075. https://doi.org/10.3390/membranes12111075
22. Kummamuru, N.B., Ciocarlan, R.G., Houlleberghs, M., Martens, J., Breynaert, d.E., Verbruggen, d.S.W., Cool, P., & Perreault, P. (2024). Surface modification of mesostructured cellular foam to enhance hydrogen storage in binary THF/H_2 clathrate hydrate. *Sustainable Energy & Fuels*, 8(13), 2791-2992. https://doi.org/10.1039/d4se00114a
23. Agustian, J., & Hermida, L. (2025). Salt-assisted mesostructured cellular foam (MCF) silica synthesis from bagasse bottom ash for enzymatic starch hydrolysis. *Bulletin of Chemical Reaction Engineering & Catalysis*, 20(3), 428-440. https://doi.org/10.9767/bcrec.20379
24. Choi, Y., Lee, J., & Kim, J. (2015). Salt-assisted synthesis of mesostructured cellular foams consisting of small primary particles with enhanced hydrothermal stability. *Microporous and Mesoporous Materials*, 212, 66–72. https://doi.org/10.1016/j.micromeso.2015.03.029
25. Milosavic, N., Prodanović, R., Jovanović, S., & Vujčić, Z. (2007). Immobilization of glucoamylase via its carbohydrate moiety on macroporous poly(GMA-co-EGDMA). *Enzyme and Microbial Technology*, 40(5), 1422–1426. https://doi.org/10.1016/j.enzmictec.2006.10.018
26. Zarina, Y., Mustafa, M., Bakri, A., Kamarudin H., Nizar K., & Rafiza A.R. (2013). Effect of preliminary calcinations on the properties of boiler ash for geopolymer composite. *Australian Journal of Basic and Applied Sciences*, June, 10–14. https://www.researchgate.net/publication/246547635_Effect_of_Preliminary_Calcinations_on_the_Properties_of_Boiler_Ash_for_Geopolymer_Composite#fullTextFileContent
27. Tangchirapat, W., Saeting, T., Jaturapitakkul, C., Kiattikomol, K., & Siripanichgorn, A. (2007). Use of waste ash from palm oil industry in concrete. *Waste Management*, 27, 81-88. https://doi.org/10.1016/j.wasman.2005.12.014
28. Tangchirapat, W., Jaturapitakkul, C., & Chindaprasirt, P. (2009). Use of palm oil fuel ash as a supplementary cementitious material for producing high-strength concrete. *Construction and Building Materials*, 23(7): 2641-2646. https://doi.org/10.1016/j.conbuildmat.2009.01.008
29. Sitohang, C., Kuncaka, A., & Suratman, A. (2024). Synthesis of mesoporous silica from palm oil boiler ash (MS-POBA) with addition of methyl ester sulfonate as a template for free fatty acid adsorption from crude palm oil (CPO). *Indonesia Journal of Chemistry*, 24(3), 729-741. https://doi.org/10.22146/ijc.87703
30. Kow, K.W., Mun, L.Y., & Yusoff, R. (2015). Silica gel synthesized from oil palm boiler ash. *Journal of Mineral Metal and Material Engineering,* 1, 14-18.
31. Adha, F.F., & Warsiki, E. (2023). Silica synthesis from oil palm mill boiler ash under different concentration of NaOH and extraction time. *IOP Conf. Series: Earth and Environmental Science*. IOP Institute Publishing. 1187, 012012. Institute of Physics Publishing. https://iopscience.iop.org/article/10.1088/1755-1315/1187/1/012012
32. Porrang, S., Davaran, S., Rahemi, N., Allahyari,

S., & Mostafavi, E. (2022). How advancing are mesoporous silica nanoparticles? A comprehensive review of the literature. *International Journal of Nanomedicine*, 17, 1803-1827. https://doi.org/10.2147/IJN.S353349

33. Hao, D., Hongyuan, Y., Tengfei, Z., & Qing, L. (2019). Amino-functionalized mesostructured cellular foam silica: a highly efficient and recyclable catalyst in the Knoevenagel condensation reaction. *Turkey Journal of Chemistry*, 43, 1204-1215. https://doi.org/10.3906/kim-1812-56
34. Luo, Z., Mao, D., Shen, W., Zheng, Y., & Yu, J. (2017). Preparation and characterization of mesostructured cellular foam silica supported Cu–Ce mixed oxide catalysts for CO oxidation. *RSC Advances*, 7, 9732–9743. https://doi.org/10.1039/c6ra25912j
35. Barton, T.J., Bull, L.M. Klemperer, W.G., Loy, D.A., McEnaney, B., Misono, M., Monson, P.A., Pez, G., Scherer, G.W., Vartuli, J.C., & Yaghir, O.M. (1999). Tailored Porous Materials. *Chemistry Materials*, 11, 2633-2656. https://doi.org/10.1021/cm9805929
36. Mateo, C., Palomo, J.M., Fernandez-Lorente, G., Guisan, J.M., & Fernandez-Lafuente, F. (2007). Improvement of enzyme activity, stability and selectivity via immobilization techniques. *Enzyme and Microbial Technology*, 40, 1451–1463. https://doi.org/10.1016/j.enzmictec.2007.01.018
37. Kannan, K., & Jasra R.V. (2009). Immobilization of alkaline serine endopeptidase from Bacillus licheniformis on SBA-15 and MCF by surface covalent binding. *Journal of Molecular Catalysis B: Enzymatic*, 56, 34-40. https://doi.org/10.1016/j.molcatb.2008.04.007
38. Actim. (2014). EDAC: Water soluble carbodiimide, downloaded from http://www.actim.com/ content/ view/25/1/lang,en/ on February 2014.
39. Zhang, Y., Zhao, L., Li, J., Zhang, H., Zheng, L., Cao, S., & Li, C. (2008). Template enhanced activity of lipase accommodated in siliceous mesocellular foams. *Biochemistry and Biophysics Research Communication*, 372, 650-655. https://doi.org/10.1016/j.bbrc.2008.05.089
40. Jin, Q., Jia, Q., Zhang, Y., Yang, Q., & Li, C. (2011). Hydrophobic surface induced activation of *Pseudomonas cepacia* lipase immobilized into mesoporous silica. *Langmuir*, 27, 12016-12024. https://doi.org/10.1021/la202794t
41. Derrick, M.R., Stulik, S., & Landry, J.M. (1999). Infrared Spectroscopy in Conservation Science. The Getty Conservation Institute.
42. Lambert, J.P., Gronert, S., Shurvell, H.F., & Lightner, D.A. (1998). Organic Structural Spectroscopy. 2nd Edition. Pearson Education. London.
43. Nelson, D.L., Cox, M.M. 2005. Lehninger Principles of Biochemistry. W.H. Freeman. New York.